Stem cell-conditioned medium accelerates distraction osteogenesis through multiple regenerative mechanisms

Yuji Ando, Kohki Matsubara, Jun Ishikawa, Masahito Fujio, Ryutaro Shohara, Hideharu Hibi, Minoru Ueda and Akihito Yamamoto*

Department of Oral and Maxillofacial Surgery, Nagoya University Graduate School of Medicine, 65 Tsurumai-cho, Showa-ku, Nagoya 466-8550, Japan

* Corresponding Author

Key words: distraction osteogenesis, stem cell-conditioned medium, endothelial progenitor cells, bone marrow stromal cells, secretome, cell recruitment

TEL: +81-52-744-2348

FAX: +81-52-744-2352

E-mail: akihito@med.nagoya-u.ac.jp

Abstract

Distraction osteogenesis (DO) successfully induces large-scale skeletal tissue regeneration, but it involves an undesirably long treatment period. A high-speed DO mouse model (H-DO) with a distraction speed twice that of a control DO model failed to generate new bone callus in the distraction gap. Here we demonstrate that the local administration of serum-free conditioned medium from human mesenchymal stem cells (MSC-CM) accelerated callus formation in the mouse H-DO model. Secretomic analysis identified factors contained in MSC-CM that recruit murine bone marrow stromal cells (mBMSCs) and endothelial cells/endothelial progenitor cells (EC/EPCs), inhibit inflammation and apoptosis, and promote osteoblast differentiation, angiogenesis, and cell proliferation. Functional assays identified MCP-1/-3 and IL-3/-6 as essential factors in recruiting mBMSCs and EC/EPCs. IL-3/-6 also enhanced the osteogenic differentiation of mBMSCs. MSC-CM that had been depleted of MCP-1/-3 failed to recruit mBMSCs, and consequently failed to promote callus formation. Taken together, our data suggest that MSCs produce a broad repertoire of trophic factors with tissue-regenerative activities that accelerate healing in the DO process.

Introduction

Distraction osteogenesis (DO) is used in orthopedic and craniofacial surgeries to lengthen the skeleton and reconstruct skeletal deformities [1-4]. DO procedure involves osteotomy followed by the gradual distraction of the two bone segments, which promotes neocallus formation in the gap between the segments. Neoangiogenesis and the recruitment of endogenous mesenchymal stem cells (MSCs) and osteogenic progenitors are required for large-scale DO-mediated tissue regeneration [4]. While DO provides significant clinical benefits, patients must endure a long treatment period (12 months on average) and use a large external fixator, which increases the risk of severe osteomyelitis by providing a possible entry route for pathogens. Therefore, it is desirable to reduce the duration of DO treatment.

Stem-cell transplantation is a promising regenerative therapy. The transplantation of various adult MSCs and their derivatives into damaged areas promotes tissue repair in both humans and model animals [5, 6]. Transplanted MSCs accelerate new bone formation in various preclinical animal models for bone defects, including DO models [7-11]. However, the engrafted stem cells have poor differentiation and survival rates, suggesting that they promote regeneration primarily through paracrine mechanisms [12, 13]. Stem cells secrete a broad repertoire of trophic and immunomodulatory factors, known as the secretome [14]. Recent preclinical studies have reported that the secretomes from various stem cells have considerable potential for treating such intractable diseases as acute myocardial infarction [15], fulminant hepatic failure [16], renal failure [17, 18], ischemic stroke [19], experimental autoimmune

encephalomyelitis [20], hypoxic brain injury [21], and lung injury [22]. However, little is known about the secretomic signatures of the various types of stem cells. Identifying the key factors of various secretomes and their functions in secretome-mediated repair will contribute to the development of new regenerative therapies that do not require cell transplants.

In this study, serum-free conditioned medium (CM) derived from human MSCs (MSC-CM) was locally administered into the distraction gap in a high-speed DO (H-DO) mouse model. MSC-CM promoted the recruitment of murine bone marrow stromal cells (mBMSCs) and of endothelial cells/endothelial progenitor cells (EC/EPCs), and the establishment of a neoangiogenic network. These tissue-regenerative activities accelerated neocallus formation in the DO gap.

Materials and methods

Cell culture and CM preparation

Human bone marrow MSCs and human skin fibroblasts (FBs) were cultured as recommended by the suppliers, Lonza Walkersville and Health Science Research Resources Bank Japan, respectively. Briefly, cells were cultured in DMEM (Dulbecco's modified Eagle's medium, Sigma) containing 10% fetal bovine serum (FBS) (Lonza Walkersville) at 37 °C in a 5% CO_2 atmosphere and were subcultured every 6-7 days. When the cells reached 70-80% confluence, they were placed in serum-free DMEM and incubated for 48 h at 37°C in 5% CO_2, after which the CM was collected and centrifuged for 4-5 minutes at 4 °C, 22,140 g. After brief re-centrifugation, the supernatant was collected and used as CM.

Mouse DO model

All animal experiments were performed in accordance with the Guidelines for Animal Experimentation of the Nagoya University School of Medicine. We used 8- to 10-week-old female ICR mice (Chubu Kagaku Shizai Corporation). The mouse DO model was generated and modified as previously described [23-25]. In this model, the external fixator consisted of two incomplete acrylic resin rings (outer diameter 20 mm, inner diameter 10 mm, and thickness 5 mm) and an expansion screw (600-301-30, Ortho Dentaurum). The total weight of the device, including the needles inserted into the tibia, was 2.7 g. The animals were anesthetized with an intraperitoneal injection of pentobarbital at 40 mg/kg body weight. The right limb was shaved and prepared with iodine solution. An anterior

longitudinal incision was made on the right leg and the underlying muscles were bluntly separated, taking care not to remove all of the periosteum. A fibulotomy was performed with scissors. The tibia was attached to the fixator using one pair of 25-gauge needles proximally, one pair of 27-gauge needles distally, and acrylic resin. After the resin was completely polymerized (approximately 5 min), an osteotomy was performed at the middle of the diaphysis using very small cutting forceps, and the wound was closed with a 5-0 nylon suture. Distraction began after a 3 day latency period and continued for 8 days at a rate of 0.2 mm/12 h, increasing the tibia length by 3.2 mm. The model with this 8-day distraction time is referred to as the control (C-DO) model in the rest of the paper. The mice were sacrificed 15 days after surgery.

Mouse high-speed DO model (H-DO) with cell-transplantation or CM-treatment

To determine the effect of administering MSCs or MSC-CM during DO, we created a mouse H-DO model with a distraction rate of 0.4 mm/12 h, a length increase of 3.2 mm in 4 days. In the cell-transplanted group, 3×10^5 MSCs or FBs in 20 μl phosphate-buffered saline (PBS; Sigma) were transplanted into the distraction zone on day 5. The mice were sacrificed 5, 7, or 11 days after surgery. In the CM-treated groups, 20 μl collagen gel matrix (Cellmatrix Type I-A; Nitta Gelatin) containing 20 μl serum-free DMEM (control) or FB-CM or MSC-CM was injected transcutaneously into the center of the distraction zone using a 29-gauge needle on days 3, 5 and 7. Mice were sacrificed 7 and 11 days after surgery.

Administration of specific factors into the H-DO model

Various combinations of recombinant human MCP-1, MCP-3, IL-3, and IL-6 (100 ng each; R&D Systems), in 20 μl of collagen gel matrix were injected transcutaneously into the center of the distraction zone of the H-DO model on days 3, 5, and 7. Mice were sacrificed 11 days after surgery.

Histology

After perfusing mice with a 4% paraformaldehyde solution, the DO tibial segments were harvested, embedded in SCEM gel (8091140; Leica), and frozen in cooled isopentane. Non-decalcified tibial bone sections were generated using Kawamoto's film method (8091098; Leica) [26]. Cryostat sections (5-μm thick) were stained with hematoxylin and eosin.

Histomorphometric analysis

Sections of the center and to each side of the center of the distraction gap (3 sections) were analyzed to detect bone formation. The distraction zone was defined as the area enclosed in a quadrangle with its endpoints formed by the osteotomized lines (Fig 1C). The percentage of callus (new bone zone) within the distraction zone [11] was calculated from digital images obtained with ImageJ software (http://rsb.info.nih.gov/ij/). Some new bone formed outside the DO gap, indicating that our statistical data might underestimate the callus formation activity under some conditions. However, because the mechanisms underlying

the new callus formation occurring outside the DO gap were unclear, we only evaluated the callus formation activity expressed in the DO gap in this study.

Immunohistochemistry

Samples were sectioned at 5 μm, fixed in 99.5% ethanol for 10 min at room temperature, washed, blocked with 5% bovine serum albumin/PBS for 30 min, and stained with primary antibodies in blocking buffer for 1 h. The sections were then stained with secondary antibodies for 30 min, mounted with an SCMM R3 (Leica), and examined with a BZ9000 fluorescence microscope (Keyence). The following antibodies were used for immunostaining: rabbit monoclonal antibody (mAb) against human major histocompatibility complex class I (human MHC class I) (ab52922; Abcam), rat mAb against stem cell antigen-1 (Sca-1) (D7; BD Pharmingen), rabbit mAb against platelet-derived growth factor receptor alpha (PDGFRα) (D1E1E; Cell Signaling Technology), rat mAb against CD31 (390; eBioscience), and rabbit mAb against alpha smooth muscle actin (αSMA) (04-1094; Millipore) and rat mAb CD11b (M1/70; eBioscience). Secondary antibodies were conjugated with Alexa Fluor 488 or 555 (Invitrogen). Cell nuclei were labeled with 4',6-diamidino-2-phenylindole (DAPI) (Invitrogen) and were counted in randomly selected fields (size of analyzed field; 310×410 μm). Positively stained MHC class I cells and CD11b cells were counted in each field of view (FOV). The microvessel supply was assessed by measuring the number and density of CD31-positive cells around muscle fibers, using a fluorescence microscope (BZ9000).

Cytokine antibody assay

Cytokine antibody array experiments were conducted at Filgen, Incorporated (Nagoya, Japan) using the RayBio Human Cytokine Antibody Array G Series 4000 (Applied arrays; RayBiotech, Inc.). Cytokines in the MSC-CM and serum-free DMEM were detected using 274-human-cytokine array plates, by laser scanning. All the scans were carried out in duplicate. The data obtained with DMEM represent the assay background and were subtracted before analysis. The data were normalized to the values of positive controls provided by the manufacturer.

Measurement of cytokines in MSC-CM, and protein depletion assays

We measured the FB-CM and MSC-CM levels of C-C motif chemokine 2/monocyte chemoattractant protein-1 (CCL2/MCP-1), C-C motif chemokine 7/monocyte chemoattractant protein-3 (CCL7/MCP-3), Interleukin-3 (IL-3), Interleukin-6 (IL-6), and Stromal-cell-derived factor-1 (SDF-1) using an ELISA kit (Human CCL2/MCP-1, Human CCL-7/MCP-3, Human IL-3, Human IL-6 and Human CXCL12/SDF-1 alpha Quantikine ELISA Kit; R&D Systems). MSC-CM was depleted of MCP-1 and MCP-3 (MCP-1/-3) by adding anti-MCP-1 and anti-MCP-3 neutralizing antibodies (R&D Systems), pre-attached to Protein G Sepharose (GE Healthcare), and incubating the mixture overnight at 4 °C. The antibody beads were removed by centrifugation (MSC-CM-MCP-1/-3), and the depletion of MCP-1/-3 was confirmed by ELISA. The control CM was treated the same way, except an anti-SDF-1 antibody of the same Ig subtype

(MSC-CM-SDF-1) was attached to the beads.

Isolation of mouse bone marrow mononuclear cells (mBMMNCs)

mBMMNCs were collected from the femurs of 8- to 10-week-old female ICR mice using an established protocol [27]. In brief, mice were euthanized with CO_2, the bone marrow cavity of the proximal femur was exposed, and the marrow was flushed out with saline. Aspirations were layered onto Ficoll (Ficoll-Paque PREMIUM; GE Healthcare) and centrifuged to obtain a buffy coat between the plasma and erythrocyte components. The cell layer was recovered, washed in PBS, and centrifuged again to remove Ficoll. The cells were re-suspended in DMEM with 10% FBS.

Migration studies

Human umbilical vein endothelial cells (HUVECs) were purchased from Lonza Walkersville. The migration abilities of mBMMNCs and HUVECs in response to MSC-CM were assessed using transwell membrane chambers (pore size 8 μm; BD Falcon; BD) as previously described [27, 28]. Briefly, mBMMNCs or HUVECs were seeded into the upper chambers of the membranes at a density of 1×10^5 cells/well in 700 μl serum-free DMEM, and 1400 μl of serum-free DMEM (control), MSC-CM, or MSC-CM with neutralizing antibodies was added to the lower chamber. Cells were incubated for 16 h (mBMMNCs) or 8 h (HUVEC) at 37 °C in 5% CO_2/95% air. Neutralizing antibodies against human MCP-1, MCP-3, IL-3, IL-6, Regulated upon activation normal T-cell expressed and secreted (RANTES/CCL5) or SDF-1 (10 μg/ml each; R&D Systems) were added to the

lower chamber. SDF-1 was used as a control antibody. The membranes were fixed in a 4% paraformaldehyde solution and stained with hematoxylin. Non-migratory cells on the upper chamber were removed with cotton swabs. For each test medium, cells that had migrated to the lower side of the membrane were counted using an inverted microscope.

Osteoblast differentiation

KUM9 cells (multipotential progenitor cells derived from mBMSCs) [29] were plated at 3×10^4 cells/well into 24-well plates for the alkaline phosphatase (ALP) activity assay. DMEM (control), MSC-CM, and MSC-CM containing neutralizing antibodies against human IL-3, IL-6, RANTES, or SDF-1 (10 μg/ml each: R&D Systems) were used as test media. Equal numbers of mBMSCs were incubated with osteogenic supplements (10% FBS, 10 mM β-glycerophosphate, 50 μg/ml ascorbic acid, and 100 nM dexamethasone) in DMEM or MSC-CM, and the medium was exchanged three times each week. After 7 days of mBMSC induction culture, the protein level was determined with the BCA Protein Assay Reagent Kit (Thermo Fisher Scientific Pierce Biotechnology), and the ALP activity was determined by measuring the absorbance at 415 nm to detect p-nitro-phenyl phosphate (SensoLyte pNPP Alkaline Phosphatase Assay Kit; AnaSpec). The cellular alkaline phosphatase activity was determined as previously described [30] and normalized to the protein concentration. Data are expressed as the micromoles of inorganic phosphate cleaved by alkaline phosphatase in 30 minutes per μg of protein.

After 14 days of induction culture, mBMSCs were fixed and stained with Alizarin red-S to detect mineralized nodules formed in vitro, as described previously [31]. Briefly, the cells were fixed in 4% paraformaldehyde and incubated with Alizarin red-S (40 mM, pH 6.4; Sigma) for 10 minutes at room temperature. After washing the wells with distilled water, the plates were photographed. The Alizarin red dye was then extracted with 10% formic acid, and the absorbance at 415 nm was determined with a microplate reader and normalized to the protein concentration.

Quantification and statistical analysis

Cells expressing a particular marker or combination of markers were counted with fluorescence microscopy (BZ9000) and ImageJ software. The SPSS statistical package was used for statistical analysis. Comparisons were made using Student's t-test or Tukey's post hoc test. Results were expressed as the mean ± standard deviation (SD: $p < 0.05$ was considered statistically significant).

Results

Engrafted MSCs promote new bone callus in DO by paracrine mechanisms

The feasibility of DO-mediated tissue regeneration is determined by the distraction rate. High- and low-speed traction cause premature and impaired ossification, respectively, in the gap [32-34]. We designed an H-DO model in which the bone fragments were distracted at 0.4 mm per 12 h, which was twice as fast as in the C-DO model (Fig. 1A). At the end of the consolidation period, the C-DO gap was filled with new bone callus, while the H-DO gap was filled with fibrotic tissue (Figs. 1B and C). Notably, we frequently observed failed callus formation at the distal end of the gap, while that at the proximal end was less affected by the H-DO procedure. As described previously, engrafted MSCs, but not FBs, promoted callus formation in the H-DO gap [9-11] (Figs. 1D and E). However, immunohistochemical analysis with a human MHC class I-specific antibody (Fig. 1I) showed that the engrafted MSCs had disappeared from the DO gap by the end of the consolidation period (Fig. 1J), indicating that the engrafted MSCs accelerated callus formation by paracrine mechanisms. This notion was further supported by the finding that callus formation was enhanced in the H-DO gaps treated with MSC-CM, but not in those treated with DMEM or FB-CM (Figs. 1F-H). Measurements of the osteoid area showed that the osteogenic activity was similar in the H-DO distraction gaps treated with MSC-CM or with transplanted MSCs (Fig. 1K). We found some callus formation outside of the DO gap (Table S1), however the relative amount of it comparing with that occurred in the gap was not significant (Table S1).

MSC-CM accelerates endogenous murine BMSC recruitment and blood vessel formation

We hypothesized that endogenous MSCs and EC/EPCs contribute to the DO-mediated tissue regeneration, and that MSC-CM accelerates the recruitment of these cells to the distraction gap. mBMSCs that express both Sca-1 and PDGFRα are known to have a robust potential to differentiate into osteoblasts [35]. The recruitment of both Sca-1$^+$/PDGFR-α$^+$ mBMSCs and CD31$^+$ EC/EPCs was increased in the C-DO, but not the H-DO gap (Fig. 2M for mBMSCs and [25] for EC/EPCs), and was restored in the H-DO gap by MSC-CM treatment (Figs. 2A-F, G, J, N, and O). Furthermore, 7 days after the operation, a large number of mature blood vessels composed of CD31$^+$ ECs and αSMA$^+$ pericytes had appeared in the H-DO gap in the MSC-CM group (Figs. 2G-L). Statistical analysis revealed that the number and area of mature vessels in the H-DO gap treated with MSC-CM were 1.6 and 1.5 times those of the DMEM group, respectively (Figs. 2P and Q). Thus, MSC-CM treatment promoted both the recruitment of mBMSCs and EC/EPCs and the formation of mature blood vessels, thereby restoring callus formation in the H-DO distraction gap.

MSC-CM secretome analysis

Cytokine antibody array analysis of the soluble factors in MSC-CM yielded 43 proteins with levels at least 1.5-times higher than those found in the control DMEM background (Fig. 3B). Of these, 10 were proteins known to be involved in such tissue-regenerating mechanisms as the recruitment of MSCs and EC/EPCs, osteoblast differentiation, angiogenesis, cell proliferation, and inflammation

suppression (Fig. 3A). Based on these proteins' reported functions, we assumed that MCP-1/-3 and RANTES recruit mBMMNCs, while IL-3/-6 recruit EC/EPCs and enhance osteogenetic activity. ELISA analysis revealed that MSC-CM contained these factors at picogram levels (Table 1).

Factors in MSC-CM recruit stem/progenitor cells and promote osteogenic differentiation

Transwell migration assays showed that, for mBMMNCs and HUVECs, MSC-CM was more chemoattractive than DMEM. Neutralizing antibodies against MCP-1 and MCP-3, but not IL-3, IL-6, RANTES, or SDF-1, strongly inhibited the MSC-CM-mediated mBMMNC migration (Fig. 4A). On the other hand, neutralizing antibodies against IL-3 or IL-6, but not MCP-1, MCP-3, RANTES, or SDF-1, significantly suppressed the HUVEC migration (Fig. 4B).

The immortalized mBMSC cell line KUM9, when treated with MSC-CM together with osteoblast differentiation supplements (see Materials and Methods) exhibited increased ALP activity (Fig. 5A) and strong Alizarin red-S staining (Figs. 5B and C). This MSC-CM-induced mineralization was inhibited by antibodies against IL-3 or IL-6, but not RANTES or SDF-1, indicating that MSC-CM promoted the ossification of mBMSCs though both IL-3 and IL-6 signaling.

MSC-CM depleted of MCP-1/-3 failed to recruit mBMSCs or to restore bone callus formation

We next analyzed the role of MSC-CM-mediated mBMSC recruitment in DO-mediated tissue regeneration. We found that new bone callus failed to form in

the distal end of H-DO gaps treated with MSC-CM that had been immunodepleted of both MCP-1 and MCP-3 (MSC-CM-MCP-1/-3), but not of SDF-1 (Figs. 6A-D). Immunohistochemical analysis showed that the integration of mBMSCs, but not EC/EPCs, was significantly impaired when the gap was treated with MSC-CM-MCP-1/-3 as opposed to MSC-CM (Figs. 6E-G). There was no significant difference between the number of mBMSCs in the gaps treated with DMEM (Figure 2N; 17.1 ± 5.2/mm^2) and MSC-CM-MCP-1/-3 (Figure 6E; 21.9 ± 2.4/mm^2, p=0.104). These results demonstrated that the MSC-CM-mediated recruitment of mBMSCs plays an important role in accelerating DO-mediated tissue regeneration.

Discussion

While a shorter DO treatment period would provide significant clinical benefits, insufficient callus formation in the distraction gap is a problem in H-DO. In our H-DO model, the callus formation at the distal end of the H-DO gap was frequently impaired. Our observations indicated that the tissue regeneration condition of the distal end was more severe than that at the proximal end and that therapeutic intervention was required to restore the tissue regeneration activity of the H-DO. This study demonstrated that when locally administered into the H-DO gap, MSC-CM promoted new bone callus formation at the distal end of the gap by accelerating the recruitment of endogenous mBMSCs and EC/EPCs. Secretome analysis of MSC-CM found 10 tissue-regenerating trophic factors that are known to be involved in the recruitment of BMSCs and EC/EPCs as well as in osteoblast differentiation, angiogenesis, cell proliferation, and inflammation suppression

(Fig. 3A). Taken together, these findings reveal a novel application of MSC-CM for enhancing the clinical efficiency of DO for correcting unequal limb length, severe deformities, and bone defects.

Tissue regeneration requires the recruitment of endogenous stem/progenitor cells to the target site [5, 6, 36-38], where they promote the formation of new blood vessels that transport oxygen, nutrients, trophic factors, and various cells that are essential to tissue repair [39-41]. MSCs can differentiate into various tissue-specific cell types according to the disease circumstances, and their trophic activities promote vascularization and suppress inflammatory responses [5, 6]. A high DO distraction rate suppresses the recruitment of EC/EPCs toward the gap, severely decreasing neovessel formation and increasing the fibrous zone [32, 33]. H-DO also suppressed the recruitment of Sca-1^{+}/PDGFRα^{+} mBMSCs, which have high osteogenic activity (Fig. 2M). Thus, a primary cause of H-DO's failure to regenerate tissue in the distraction gap is the defective integration of both endothelial and osteogenic progenitor cells. Our data show that MSC-CM treatment recovered the recruitment of both endothelial and osteogenic progenitors. Furthermore, when the gap was treated with MSC-CM that had been specifically depleted of the MSC-homing factors MCP-1 and MCP-3, few if any Sca-1^{+}/PDGFRα^{+} mBMSCs were recruited and consequently, the callus formation in the gap was deficient. Thus, the recruitment of stem/progenitor cells is an essential mechanism by which MSC-CM restored the callus formation in H-DO.

Among several tissue-regenerating factors that are secreted by MSCs, we identified MCP-1/-3 and IL-3/-6 as homing factors for mBMSCs and EC/EPCs,

respectively. We also observed that IL-3/-6 was able to promote the osteogeneic differentiation of mBMSCs. These results suggest that MCP-1/-3 and IL-3/-6 act in concert to accelerate callus formation. However, in our preliminary experiments, various combinations of MCP-1/-3 and IL-3/-6 alone could not restore callus formation (Fig. S1A). Notably, these factors are known to be major players in the pro-inflammatory immune responses. For instance, MCP-1 accelerates inflammation by recruiting immune cells, including macrophages, monocytes, leucocytes, memory T lymphocytes, and natural killer (NK) cells [42-44]. IL-6 accelerates inflammation by promoting the differentiation of cytotoxic T cells and Th17 cells [45]. Indeed, our histological analyses revealed a prominent accumulation of $CD11b^+$ mononuclear immune cells in the DO gaps treated with MCP-1/-3 and IL-3/-6 (Figs. S1B-D), suggesting that these factors can exert both detrimental and beneficial effects in tissue regeneration. We speculate that immunosuppressive factors in the MSC-CM may counteract the pro-inflammatory properties of MCP-1/-3 and IL-3/-6 and enhance their regenerative activities, thereby significantly enhancing callus formation in the H-DO gap. Clarifying MSC-CM's immunosuppressive mechanisms will advance our understanding of MSC-CM-mediated tissue regeneration.

Engrafted MSCs promote bone regeneration both by replacing damaged cells and by trophic and paracrine mechanisms [6]. However, the poor differentiation and survival of engrafted stem cells, both in our data and in previous studies, suggests that the regenerative properties of these cells are exerted primarily through paracrine mechanisms [12, 13]. This finding led us to examine the regenerative activity of paracrine factors secreted by MSCs. In the

present study, these factors were harvested in a serum-free cell culture. MSCs express significantly higher levels of several arteriogenic cytokines when subjected to hypoxic stress [28, 46, 47]. When deprived of serum, starvation stress induces MSCs to secrete angiogenic factors [48]. In general, severe stress causes cells to activate survival pathways and secrete factors to counteract toxic conditions [49, 50]. Thus, severe stress conditions may significantly increase the therapeutic efficiency of factors harvested in the MSC-CM. A serum-free condition also increases the purity of the harvested factors. Although only small amounts of each factor are contained in the MSC-CM, multiple regenerative factors may cooperate to accelerate tissue regeneration. Although BMSC transplantation accelerates callus formation, immune rejection by the allogeneic response and unexpected tumor formation are serious concerns with this procedure. In contrast, CM-treatment can deliver the paracrine/tropic tissue-regenerative activities of stem cells without these concerns. Thus, MSC-CM may be a key component in the development of practical, efficient therapies to regenerate skeletal tissues.

In summary, our data show that MSC-CM accelerates the formation of new bone callus, thus shortening the time period required for DO treatment. MSC-CM recruits endogenous mBMSCs and EC/EPCs via MCP-1/-3 and IL-3/-6 signaling, respectively, and this trafficking of stem/progenitor cells is essential for MSC-CM-mediated callus formation. We believe that our findings begin to elucidate how multiple classes of factors contained in MSC-CM cooperate to promote bone regeneration.

Acknowledgments

We thank Drs. Kiyoshi Sakai, Masayuki Ikeno, Kazuhiko Kinoshita, Ms. Mami Naruse, and the members of the Department of Oral and Maxillofacial Surgery for their encouragement to complete this study. We also thank the Division of Experimental Animals and Medical Research Engineering, Nagoya University Graduate School of Medicine, for the housing of mice and for microscope maintenance. This work was supported by Grants-in-Aid for Scientific Research on Priority Areas from the Ministry of Education, Culture, Sports, Science and Technology of Japan and COE for education and research of Micro-Nano Mechatronics Nagoya University Global COE Program.

References

[1] Ilizarov GA. Clinical application of the tension-stress effect for limb lengthening. Clin Orthop Relat Res 1990: 8-26.

[2] McCarthy JG, Stelnicki EJ, Mehrara BJ, Longaker MT. Distraction osteogenesis of the craniofacial skeleton. Plast Reconstr Surg 2001;107: 1812-27.

[3] Samchukov ML, Makarov MR, Cherkashin AM, Birch JG. Distraction Osteogenesis of the Orthopedic Skeleton: Basic Principles and Clinical Applications; 2008.

[4] Ai-Aql ZS, Alagl AS, Graves DT, Gerstenfeld LC, Einhorn TA. Molecular mechanisms controlling bone formation during fracture healing and distraction osteogenesis. J Dent Res 2008;87: 107-18.

[5] Uccelli A, Moretta L, Pistoia V. Mesenchymal stem cells in health and disease. Nat Rev Immunol 2008;8: 726-36.

[6] Tolar J, Le Blanc K, Keating A, Blazar BR. Concise review: hitting the right spot with mesenchymal stromal cells. Stem cells 2010;28: 1446-55.

[7] Bruder SP, Jaiswal N, Ricalton NS, Mosca JD, Kraus KH, Kadiyala S. Mesenchymal stem cells in osteobiology and applied bone regeneration. Clin Orthop Relat Res 1998: S247-56.

[8] Takamine Y, Tsuchiya H, Kitakoji T, Kurita K, Ono Y, Ohshima Y, Kitoh H, Ishiguro N, Iwata H. Distraction osteogenesis enhanced by osteoblastlike cells

and collagen gel. Clin Orthop Relat Res 2002: 240-6.

[9] Kitoh H, Kitakoji T, Tsuchiya H, Katoh M, Ishiguro N. Distraction osteogenesis of the lower extremity in patients with achondroplasia/hypochondroplasia treated with transplantation of culture-expanded bone marrow cells and platelet-rich plasma. J Pediatr Orthop 2007;27: 629-34.

[10] Kitoh H, Kitakoji T, Tsuchiya H, Katoh M, Ishiguro N. Transplantation of culture expanded bone marrow cells and platelet rich plasma in distraction osteogenesis of the long bones. Bone 2007;40: 522-8.

[11] Kinoshita K, Hibi H, Yamada Y, Ueda M. Promoted new bone formation in maxillary distraction osteogenesis using a tissue-engineered osteogenic material. J Craniofac Surg 2008;19: 80-7.

[12] Kotobuki N, Katsube Y, Katou Y, Tadokoro M, Hirose M, Ohgushi H. In vivo survival and osteogenic differentiation of allogeneic rat bone marrow mesenchymal stem cells (MSCs). Cell Transplant 2008;17: 705-12.

[13] Zimmermann CE, Gierloff M, Hedderich J, Acil Y, Wiltfang J, Terheyden H. Survival of transplanted rat bone marrow-derived osteogenic stem cells in vivo. Tissue engineering. Part A 2011;17: 1147-56.

[14] Ranganath SH, Levy O, Inamdar MS, Karp JM. Harnessing the mesenchymal stem cell secretome for the treatment of cardiovascular disease. Cell stem cell 2012;10: 244-58.

[15] Timmers L, Lim SK, Arslan F, Armstrong JS, Hoefer IE, Doevendans PA, Piek JJ, El Oakley RM, Choo A, Lee CN, Pasterkamp G, de Kleijn DP. Reduction of myocardial infarct size by human mesenchymal stem cell conditioned medium. Stem Cell Res 2007;1: 129-37.

[16] Parekkadan B, van Poll D, Suganuma K, Carter EA, Berthiaume F, Tilles AW, Yarmush ML. Mesenchymal stem cell-derived molecules reverse fulminant hepatic failure. PLoS One 2007;2: e941.

[17] Bi B, Schmitt R, Israilova M, Nishio H, Cantley LG. Stromal cells protect against acute tubular injury via an endocrine effect. J Am Soc Nephrol 2007;18: 2486-96.

[18] van Koppen A, Joles JA, van Balkom BW, Lim SK, de Kleijn D, Giles RH, Verhaar MC. Human embryonic mesenchymal stem cell-derived conditioned medium rescues kidney function in rats with established chronic kidney disease. PLoS One 2012;7: e38746.

[19] Cho YJ, Song HS, Bhang S, Lee S, Kang BG, Lee JC, An J, Cha CI, Nam DH, Kim BS, Joo KM. Therapeutic effects of human adipose stem cell-conditioned medium on stroke. J Neurosci Res 2012;90: 1794-802.

[20] Bai L, Lennon DP, Caplan AI, DeChant A, Hecker J, Kranso J, Zaremba A, Miller RH. Hepatocyte growth factor mediates mesenchymal stem cell-induced recovery in multiple sclerosis models. Nat Neurosci 2012;15: 862-70.

[21] Yamagata M, Yamamoto A, Kako E, Kaneko N, Matsubara K, Sakai K,

Sawamoto K, Ueda M. Human dental pulp-derived stem cells protect against hypoxic-ischemic brain injury in neonatal mice. Stroke 2013;44: 551-4.

[22] Ionescu L, Byrne RN, van Haaften T, Vadivel A, Alphonse RS, Rey-Parra GJ, Weissmann G, Hall A, Eaton F, Thebaud B. Stem cell conditioned medium improves acute lung injury in mice: in vivo evidence for stem cell paracrine action. Am J Physiol Lung Cell Mol Physiol 2012;303: L967-77.

[23] Tay BK, Le AX, Gould SE, Helms JA. Histochemical and molecular analyses of distraction osteogenesis in a mouse model. J Orthop Res 1998;16: 636-42.

[24] Isefuku S, Joyner CJ, Simpson AH. A murine model of distraction osteogenesis. Bone 2000;27: 661-5.

[25] Fujio M, Yamamoto A, Ando Y, Shohara R, Kinoshita K, Kaneko T, Hibi H, Ueda M. Stromal cell-derived factor-1 enhances distraction osteogenesis-mediated skeletal tissue regeneration through the recruitment of endothelial precursors. Bone 2011;49: 693-700.

[26] Kawamoto T. Use of a new adhesive film for the preparation of multi-purpose fresh-frozen sections from hard tissues, whole-animals, insects and plants. Arch Histol Cytol 2003;66: 123-43.

[27] Watson SL, Marcal H, Sarris M, Di Girolamo N, Coroneo MT, Wakefield D. The effect of mesenchymal stem cell conditioned media on corneal stromal fibroblast wound healing activities. Br J Ophthalmol 2010;94: 1067-73.

[28] Chen L, Tredget EE, Wu PY, Wu Y. Paracrine factors of mesenchymal stem cells recruit macrophages and endothelial lineage cells and enhance wound healing. PLoS One 2008;3: e1886.

[29] Matsumoto S, Shibuya I, Kusakari S, Segawa K, Uyama T, Shimada A, Umezawa A. Membranous osteogenesis system modeled with KUSA-A1 mature osteoblasts. Biochim Biophys Acta 2005;1725: 57-63.

[30] Cho TJ, Kim JA, Chung CY, Yoo WJ, Gerstenfeld LC, Einhorn TA, Choi IH. Expression and role of interleukin-6 in distraction osteogenesis. Calcif Tissue Int 2007;80: 192-200.

[31] Miyazaki T, Miyauchi S, Tawada A, Anada T, Matsuzaka S, Suzuki O. Oversulfated chondroitin sulfate-E binds to BMP-4 and enhances osteoblast differentiation. J Cell Physiol 2008;217: 769-77.

[32] Li G, Simpson AH, Kenwright J, Triffitt JT. Assessment of cell proliferation in regenerating bone during distraction osteogenesis at different distraction rates. J Orthop Res 1997;15: 765-72.

[33] Li G, Simpson AH, Kenwright J, Triffitt JT. Effect of lengthening rate on angiogenesis during distraction osteogenesis. J Orthop Res 1999;17: 362-7.

[34] Richards M, Kozloff KM, Goulet JA, Goldstein SA. Increased distraction rates influence precursor tissue composition without affecting bone regeneration. J Bone Miner Res 2000;15: 982-9.

[35] Morikawa S, Mabuchi Y, Kubota Y, Nagai Y, Niibe K, Hiratsu E, Suzuki S,

Miyauchi-Hara C, Nagoshi N, Sunabori T, Shimmura S, Miyawaki A, Nakagawa T, Suda T, Okano H, Matsuzaki Y. Prospective identification, isolation, and systemic transplantation of multipotent mesenchymal stem cells in murine bone marrow. The Journal of experimental medicine 2009;206: 2483-96.

[36] Karp JM, Leng Teo GS. Mesenchymal stem cell homing: the devil is in the details. Cell stem cell 2009;4: 206-16.

[37] Marsell R, Einhorn TA. The biology of fracture healing. Injury 2011;42: 551-5.

[38] Shirley D, Marsh D, Jordan G, McQuaid S, Li G. Systemic recruitment of osteoblastic cells in fracture healing. J Orthop Res 2005;23: 1013-21.

[39] Matsumoto T, Mifune Y, Kawamoto A, Kuroda R, Shoji T, Iwasaki H, Suzuki T, Oyamada A, Horii M, Yokoyama A, Nishimura H, Lee SY, Miwa M, Doita M, Kurosaka M, Asahara T. Fracture induced mobilization and incorporation of bone marrow-derived endothelial progenitor cells for bone healing. J Cell Physiol 2008;215: 234-42.

[40] Lee DY, Cho TJ, Kim JA, Lee HR, Yoo WJ, Chung CY, Choi IH. Mobilization of endothelial progenitor cells in fracture healing and distraction osteogenesis. Bone 2008;42: 932-41.

[41] Asahara T, Kawamoto A, Masuda H. Concise review: Circulating endothelial progenitor cells for vascular medicine. Stem cells 2011;29: 1650-5.

[42] Bachmann MF, Kopf M, Marsland BJ. Chemokines: more than just road

signs. Nat Rev Immunol 2006;6: 159-64.

[43] Yadav A, Saini V, Arora S. MCP-1: chemoattractant with a role beyond immunity: a review. Clin Chim Acta 2010;411: 1570-9.

[44] Deshmane SL, Kremlev S, Amini S, Sawaya BE. Monocyte chemoattractant protein-1 (MCP-1): an overview. J Interferon Cytokine Res 2009;29: 313-26.

[45] Nishimoto N. Interleukin-6 as a therapeutic target in candidate inflammatory diseases. Clin Pharmacol Ther 2010;87: 483-7.

[46] Ohnishi S, Yasuda T, Kitamura S, Nagaya N. Effect of hypoxia on gene expression of bone marrow-derived mesenchymal stem cells and mononuclear cells. Stem Cells 2007;25: 1166-77.

[47] Kinnaird T, Stabile E, Burnett MS, Lee CW, Barr S, Fuchs S, Epstein SE. Marrow-derived stromal cells express genes encoding a broad spectrum of arteriogenic cytokines and promote in vitro and in vivo arteriogenesis through paracrine mechanisms. Circ Res 2004;94: 678-85.

[48] Oskowitz A, McFerrin H, Gutschow M, Carter ML, Pochampally R. Serum-deprived human multipotent mesenchymal stromal cells (MSCs) are highly angiogenic. Stem Cell Res 2011;6: 215-25.

[49] Strum JC, Johnson JH, Ward J, Xie H, Feild J, Hester A, Alford A, Waters KM. MicroRNA 132 regulates nutritional stress-induced chemokine production through repression of SirT1. Mol Endocrinol 2009;23: 1876-84.

[50] Lee SH, Lee YJ, Song CH, Ahn YK, Han HJ. Role of FAK phosphorylation in hypoxia-induced hMSCS migration: involvement of VEGF as well as MAPKS and eNOS pathways. Am J Physiol Cell Physiol 2010;298: C847-56.

[51] Belema-Bedada F, Uchida S, Martire A, Kostin S, Braun T. Efficient homing of multipotent adult mesenchymal stem cells depends on FROUNT-mediated clustering of CCR2. Cell stem cell 2008;2: 566-75.

[52] Schenk S, Mal N, Finan A, Zhang M, Kiedrowski M, Popovic Z, McCarthy PM, Penn MS. Monocyte chemotactic protein-3 is a myocardial mesenchymal stem cell homing factor. Stem cells 2007;25: 245-51.

[53] Anton K, Banerjee D, Glod J. Macrophage-associated mesenchymal stem cells assume an activated, migratory, pro-inflammatory phenotype with increased IL-6 and CXCL10 secretion. PLoS One 2012;7: e35036.

[54] Yao JS, Zhai W, Young WL, Yang GY. Interleukin-6 triggers human cerebral endothelial cells proliferation and migration: the role for KDR and MMP-9. Biochem Biophys Res Commun 2006;342: 1396-404.

[55] Dentelli P, Del Sorbo L, Rosso A, Molinar A, Garbarino G, Camussi G, Pegoraro L, Brizzi MF. Human IL-3 stimulates endothelial cell motility and promotes in vivo new vessel formation. J Immunol 1999;163: 2151-9.

[56] Ishida Y, Kimura A, Kuninaka Y, Inui M, Matsushima K, Mukaida N, Kondo T. Pivotal role of the CCL5/CCR5 interaction for recruitment of endothelial

progenitor cells in mouse wound healing. J Clin Invest 2012;122: 711-21.

[57] Bellido T, Borba VZ, Roberson P, Manolagas SC. Activation of the Janus kinase/STAT (signal transducer and activator of transcription) signal transduction pathway by interleukin-6-type cytokines promotes osteoblast differentiation. Endocrinology 1997;138: 3666-76.

[58] Li Y, Backesjo CM, Haldosen LA, Lindgren U. IL-6 receptor expression and IL-6 effects change during osteoblast differentiation. Cytokine 2008;43: 165-73.

[59] Barhanpurkar AP, Gupta N, Srivastava RK, Tomar GB, Naik SP, Joshi SR, Pote ST, Mishra GC, Wani MR. IL-3 promotes osteoblast differentiation and bone formation in human mesenchymal stem cells. Biochem Biophys Res Commun 2012;418: 669-75.

[60] Hong KH, Ryu J, Han KH. Monocyte chemoattractant protein-1-induced angiogenesis is mediated by vascular endothelial growth factor-A. Blood 2005;105: 1405-7.

[61] McGonigle JS, Giachelli CM, Scatena M. Osteoprotegerin and RANKL differentially regulate angiogenesis and endothelial cell function. Angiogenesis 2009;12: 35-46.

[62] Cohen T, Nahari D, Cerem LW, Neufeld G, Levi BZ. Interleukin 6 induces the expression of vascular endothelial growth factor. J Biol Chem 1996;271: 736-41.

[63] Bauer SM, Bauer RJ, Liu ZJ, Chen H, Goldstein L, Velazquez OC. Vascular endothelial growth factor-C promotes vasculogenesis, angiogenesis, and collagen constriction in three-dimensional collagen gels. J Vasc Surg 2005;41: 699-707.

[64] Distler JH, Hirth A, Kurowska-Stolarska M, Gay RE, Gay S, Distler O. Angiogenic and angiostatic factors in the molecular control of angiogenesis. Q J Nucl Med 2003;47: 149-61.

[65] Wang Y, Yan W, Lu X, Qian C, Zhang J, Li P, Shi L, Zhao P, Fu Z, Pu P, Kang C, Jiang T, Liu N, You Y. Overexpression of osteopontin induces angiogenesis of endothelial progenitor cells via the avbeta3/PI3K/AKT/eNOS/NO signaling pathway in glioma cells. Eur J Cell Biol 2011;90: 642-8.

[66] Ikebuchi K, Wong GG, Clark SC, Ihle JN, Hirai Y, Ogawa M. Interleukin 6 enhancement of interleukin 3-dependent proliferation of multipotential hemopoietic progenitors. Proc Natl Acad Sci U S A 1987;84: 9035-9.

[67] Maddaluno M, Di Lauro M, Di Pascale A, Santamaria R, Guglielmotti A, Grassia G, Ialenti A. Monocyte chemotactic protein-3 induces human coronary smooth muscle cell proliferation. Atherosclerosis 2011;217: 113-9.

[68] Ouyang W, Rutz S, Crellin NK, Valdez PA, Hymowitz SG. Regulation and functions of the IL-10 family of cytokines in inflammation and disease. Annu Rev Immunol 2011;29: 71-109.

Figure legends

Figure 1. MSCs accelerate callus formation through paracrine mechanisms

(A) Distraction protocols and experimental design. After a 3-day latency period, distraction was conducted over a period of 8 days (C-DO) at 0.2 mm/12 h, or a period of 4 (H-DO) days at a rate of 4 mm/12 h (H-DO), for a total length increase of 3.2 mm. Time points: white arrowheads, MSC transplantation or CM injections. LA: latency period; AD: active distraction period; CO: consolidation period. (B-H) Representative micrographs of hematoxylin-eosin (HE)-stained DO-gap sections, shown distal (left) to proximal (right); bar = 300 μm. (C) Schematic of the distraction zone. At the end of the consolidation period, neocallus had formed in the C-DO (B) but not H-DO (C) gaps. Transplanted MSCs (E) but not FBs (D) promoted callus formation in the H-DO gap. Locally injected MSC-CM (H) but not DMEM (F) or FB-CM (G) promoted callus formation in the H-DO gap. (I) Immunohistochemical analysis of H-DO gaps: sections were prepared immediately after engrafting MSCs (post-surgery day 5) and stained with specific antibodies against human MHC class I (red) and DAPI (blue). Bar = 50 μm. (J) Quantification of transplanted human MHC class I^+ MSCs in the H-DO gap over time: MSCs had completely disappeared from the gap by the end of the consolidation period. FOV: field of view. Data represent mean ± SD; * $p < 0.05$; n = 5 per group. (K) Histomorphometric analysis of callus formation in the distraction zone at the end of the consolidation period. Note that the callus area was significantly larger in the MSC-CM groups than in the DMEM or FB-CM groups. Data represent mean ± SD; * $p < 0.05$; n = 10 per group.

Figure 2. MSC-CM accelerates the recruitment of endogenous mBMSCs and formation of blood vessels

(A-L) Representative images showing the immunohistochemical staining of H-DO gaps treated with DMEM (A-C, G-I) or MSC-CM (D-F, J-L); samples were obtained at the end of active distraction. White arrowheads (C, F) indicate mBMSCs detected with Sca-1 (green) and PDGFRα (red) staining (A-F). EC/EPCs and vascular smooth muscle cells were detected with CD31 (green) and αSMA (red) (G-L) staining, respectively. White arrowheads (I, L) indicate mature blood vessels consisting of CD31-positive endothelial cells and αSMA-positive vascular smooth muscle cells; these vessels were increased in the MSC-CM group. Bar = 50 μm. (M-O) Quantification of Sca-1$^+$/PDGFRα$^+$ mBMSCs (M and N, n = 10), CD31$^+$ EC/EPCs (O, n = 10), vessel counts (P, n = 10), and vessel density (Q, n = 10). Data represent mean ± SD; * $p < 0.05$.

Figure 3. Soluble factors contained in MSC-CM

(A) Classification of MSC-CM factors: MSC-CM contained previously annotated proteins that recruit MSCs and EC/EPCs, promote osteogenesis, angiogenesis, and cell proliferation, and inhibit inflammation. (B) Factors expressed in BMSC-CM at levels 1.5-fold or greater than those in fresh DMEM medium without cell culture. X-axis: the intensity levels of factors in MSC-CM, with the intensity of the medium control set arbitrarily as 1.0.

Figure 3 cites the following references:

[43, 51-68]

Abbreviations: MCP-1: monocyte chemoattractant protein-1; TIMP-2: tissue inhibitor of metalloproteinase-2; PAI-1: plasminogen activator inhibitor-1; beta-IG-H3: transforming growth factor beta-induced (TGFBI); IL-6: interleukin-6; IGFBP-6: insulin-like growth factor-binding protein-6; VEGF-C: vascular endothelial growth factor-C; MCP-3: monocyte chemoattractant protein-3; sTNF R1: soluble tumor necrosis factor receptor 1; TIMP-1: tissue inhibitor of metalloproteinase-1; DPP-4: dipeptidyl peptidase-4; IL-22: interleukin-22; HVEM: herpesvirus entry mediator; NAP-2: neutrophil-activating protein-2; XEDAR: X-linked ectodysplasin-A2 receptor; IL-7: interleukin-7; RANK: receptor activator of nuclear factor kappa-B; IL-3: interleukin-3; MMP-7: matrix metalloproteinase-7; RANTES: regulated upon activation normal T-cell expressed and secreted (CCL5, chemokine C-C motif ligand 5); CXCR16: chemokine C-X-C motif receptor 16; TRAIL R3: TNF related apoptosis-inducing ligand receptor 3; IL-17B: interleukin-17B; MMP-10: matrix metalloproteinase-10; LYVE-1: lymphatic vessel endothelial receptor 1; TSLP: thymic stromal lymphopoietin; NRG1-beta1, neuregulin-1-beta1.

Figure 4. Effect of MSC-CM on cell migration

The migratory response of freshly isolated mouse bone marrow mononuclear cells (mBMMNCs) (A) and HUVECs (B) to MSC-CM was measured by a modified Boyden chamber migration assay (see Materials and Methods). X-axis: migratory response relative to that for fresh DMEM medium. Neutralizing antibodies for

MCP-1/-3 and IL-3/-6, respectively, suppressed the MSC-CM-induced migration of mBMMNCs (A) and HUVECs (B). In contrast, antibodies against RANTES (CCL5) or SDF-1 (CXCL12) had little or no effect on cell migration. Triple wells were used for each treatment. Data shown represent mean ± SD of three independent experiments; * $p < 0.05$ vs DMEM, # $p < 0.05$ vs MSC-CM.

Figure 5. MSC−CM-induced mineralization in mBMSCs.

(A) The relative ALP activity of KUM9 mBMSCs. MSC-CM-OS increased the ALP activity. Triple wells were used for each treatment. Data shown represent mean ± SD of three independent experiments; *$p < 0.05$ vs DMEM-OS. (B) Representative images of KUM9 mBMSCs: those cultured in MSC-CM with osteogenic supplements (OS; see Materials and Methods) were stained more strongly by Alizarin red-S than those cultured in OS medium alone (B, C). Bar = 300 μm. MSC-CM-OS increased the Alizarin staining; this increase was suppressed by neutralizing antibodies for IL-3 and/or IL-6 (C). Triple wells were used for each treatment. Data shown represent mean ± SD of three independent experiments; *$p < 0.05$ vs DMEM-OS; # $p < 0.05$ vs MSC-CM-OS.

Figure 6. MSC-CM depleted of MCP-1/-3 failed to recruit mBMSCs or to restore callus formation in the H-DO gap

(A-C) Representative micrographs of H-DO gap sections stained with hematoxylin-eosin (HE). Bar = 300 μm. Neocallus formed in H-DO gaps treated with MSC-CM control (A) or MSC-CM depleted of SDF-1 (MSC-CM-SDF-1) (C),

but not in those treated with MSC-CM depleted of MCP-1/3 (MSC-CM-MCP-1/3) (B). (D-G) Quantification of callus formation (n = 8), the migration of Sca-1$^+$/PDGFRα$^+$ mBMSCs (n = 5) and CD31$^+$ EC/EPCs (n = 5), and vessel formation (n = 5). The specific depletion of MCP-1/3 significantly reduced the MSC-CM-mediated callus formation and mBMSC migration (D, E), but did not affect the EC/EPSC migration or vessel formation (F, G). Data represent the mean ± SD; * $p < 0.05$.

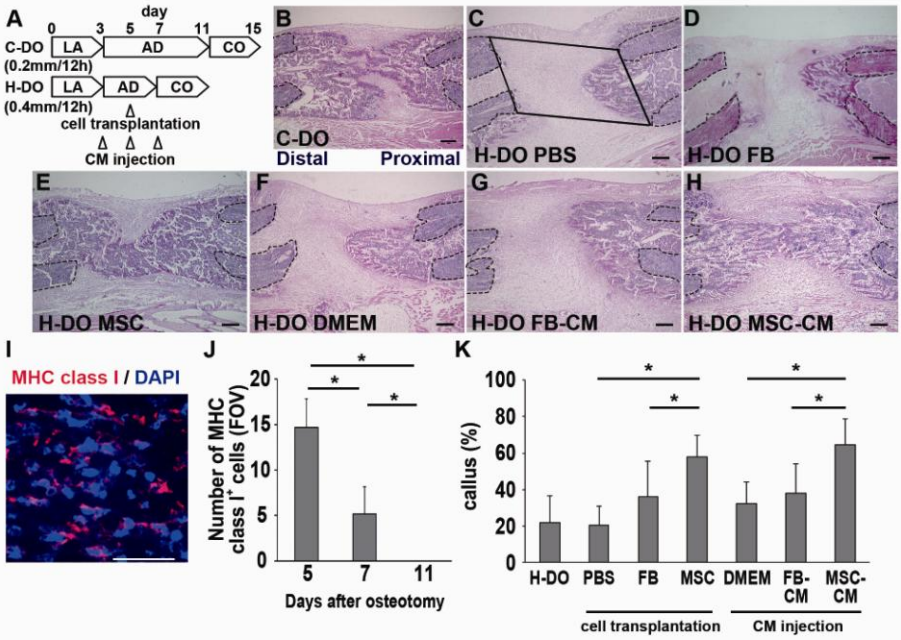

Fig1. Ando

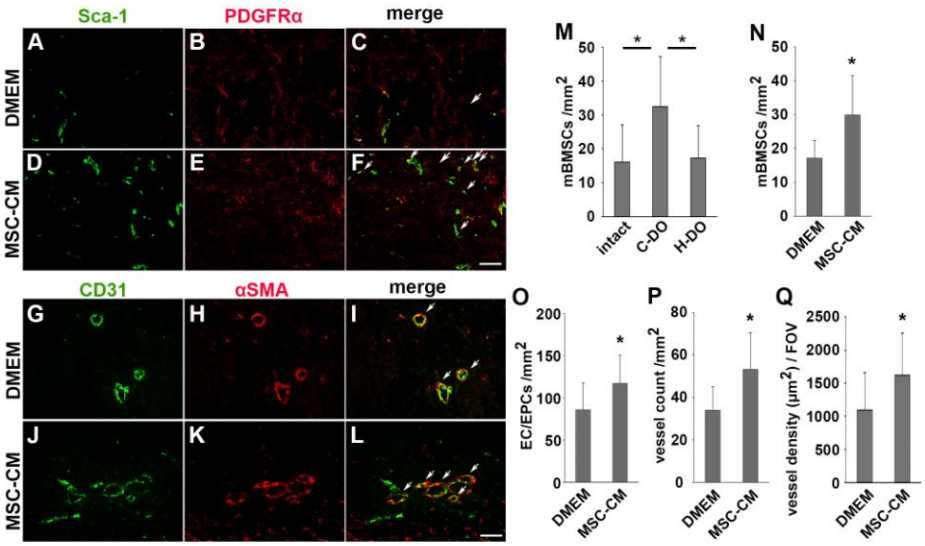

Fig 2. Ando

A

MSC recruitment	intensity	references
MCP-1	11765.7	51
MCP-3	201.0	52
RANTES	41.6	53

EC/EPC recruitment	intensity	references
IL-6	1136.7	54
IL-3	68.2	55
RANTES	41.6	56

osteogenesis	intensity	references
IL-6	1136.7	57, 58
IL-3	68.2	59

angiogenesis	intensity	references
MCP-1	11765.7	43, 60
osteoprotegerin	2236.2	61
IL-6	1136.7	62
VEGF-C	451.8	63
angiogenin	335.6	64
IL-3	68.2	55
osteopontin	63.5	65

cell proliferation	intensity	references
osteoprotegerin	2236.2	61
IL-6	1136.7	54, 66
VEGF-C	451.8	63
angiogenin	335.6	64
MCP-3	201.0	67
IL-3	68.2	55, 66
osteopontin	63.5	65

anti-inflamatation	intensity	references
IL-22	126.0	68

B

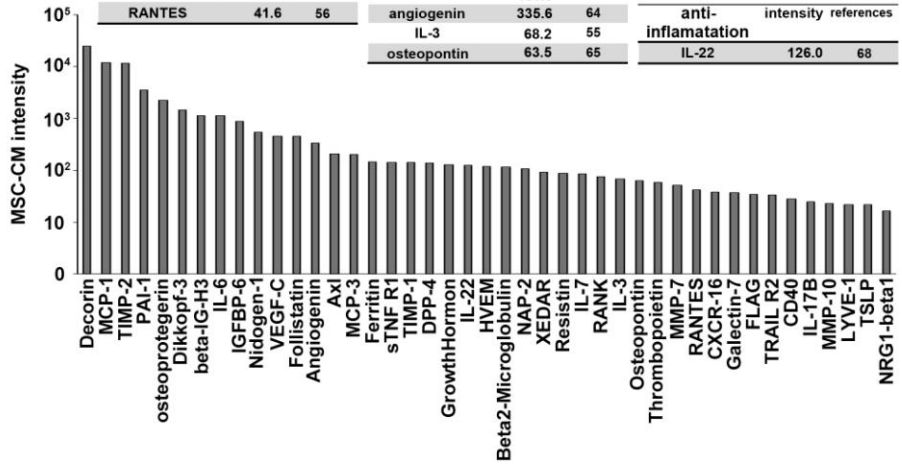

Fig 3. Ando

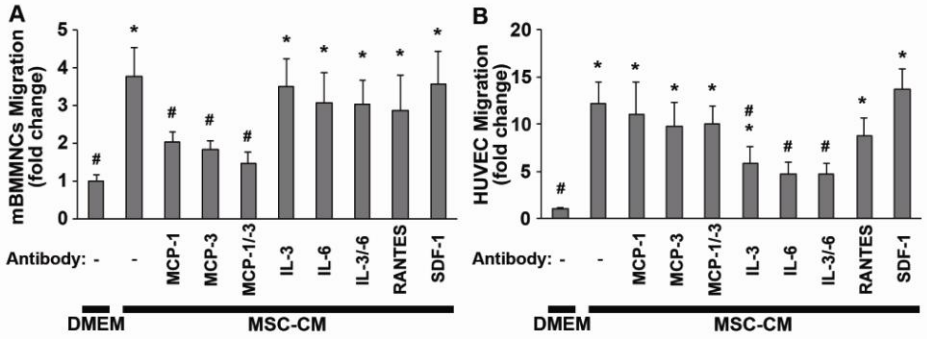

Fig 4. Ando

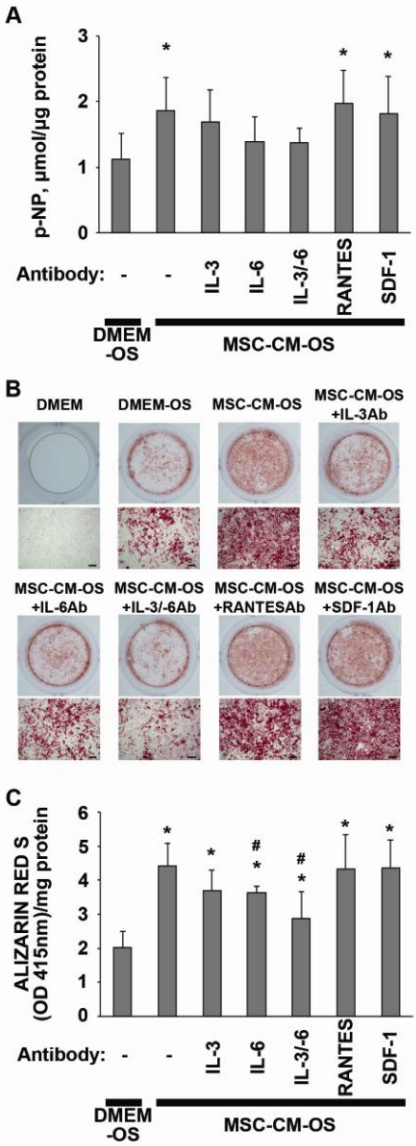

Fig 5. Ando

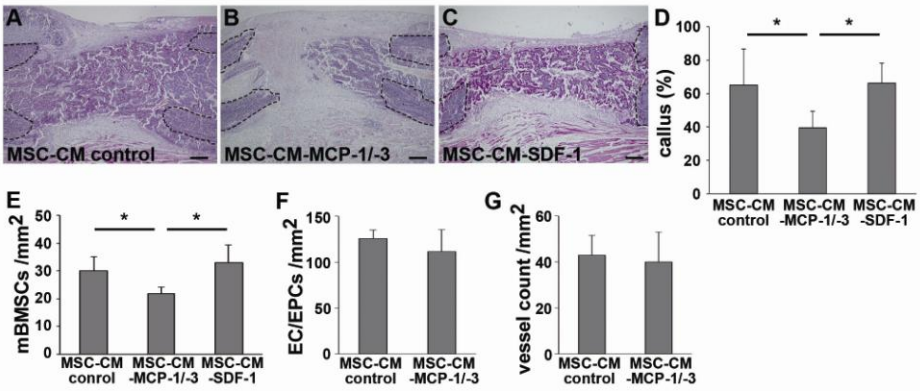

Fig 6. Ando

Table 1
Concentration of cytokines in CM (pg/ml)

Trophic factors	MSC-CM	MSC-CM control	MSC-CM-MSC-1/-3	MSC-CM-SDF-1	FB-CM
MCP-1	205±2.3	222±9.9	ND	177±9.3	70±9.7
MCP-3	102±10.9	79±9.9	ND	76±5.7	ND
IL-3	181±21.9	190±8.7	113 ±10.9	194±7.6	ND
IL-6	106±3.3	110±4.2	111±0.3	165±14.0	76±3.0
SDF-1	ND	ND	ND	ND	ND

Abbreviations: MCP-1: monocyte chemoattractant protein-1; MCP-3: monocyte chemoattractant protein-3; IL-3: interleukin-3; IL-6: interleukin-6; SDF-1: stromal-cell-derived factor-1; ND: not detected.

Research highlights

1) MSC-CM accelerates callus formation in the DO gap

2) MSC-CM promotes the recruitment of endogenous mBMSCs and EC/EPCs.

3) MSC-CM contains multiple tissue-regenerative factors.

4) MCP-1 and MCP-3 contained in MSC-CM recruit mBMSCs to the DO gap.

5) IL-3/IL-6 in MSC-CM recruits EC/EPCs and promotes mBMSC osteogenic differentiation.